Sex and age affect depot expression of calcium channels in rat white fat adipocytes.

Yan Meng, Olena. A. Fedorenko,

Maria Toledo-Rodriguez, and Paul A. Smith*

School of Life Sciences, University of Nottingham,

Queen's Medical Centre, Derby Road, Nottingham, NG7 2UH

- Corresponding Author

School of Life Sciences, University of Nottingham, Queen's Medical Centre, Derby Road, Nottingham, NG7 2UH

paul.a.smith@nottingham.ac.uk

Running title:

Sex, age, and calcium channels in fat

Word Count 4912

Key words: Sex mammogenesis fat transcriptomics

Abstract

White adipose tissue (WAT) requires extracellular Ca^{2+} influx for lipolysis, differentiation, and expansion. This partly occurs via plasma membrane Ca^{2+} voltage-dependent channels (CaVs). However, WAT exists in different depots whose function varies with age, sex, and location. To explore whether their CaV expression profiles also differ we used RNAseq and qPCR on gonadal, mesenteric, retroperitoneal, and inguinal subcutaneous fat depots from rats of different ages and sex. CaV expression was found dependent on age, gender, and WAT location. In the gonadal depots of both sexes a significantly lower expression of CaV1.2 and CaV1.3 was seen for adults compared to pre-pubescent juveniles. A lower level of expression was also seen for CaV3.1 in adult male but not female gonadal WAT; the latter of whose expression remained unchanged with age. Relatively little expression of CaV3.2 and 3.2 was observed. In post-pubescent inguinal subcutaneous fat, where mammary glands are sited, CaV3.1 was decreased in males but increased in females; data which suggests this channel is associated with mammogenesis, however no effect on intracellular Ca^{2+} levels or adipocyte size were noted. For all adult depots, CaV3.1 expression was larger in females than males; a difference not seen in pre-pubescent animals. These observations are consistent with the changes of CaV3.1 expression seenseen in 3T3-L1 cell differentiation and the ability of selective CaV3.1 antagonists to inhibit this process. Our results show that changes in CaVs expression patterns occur in fat depots related to sexual

Formatted: Superscript

dimorphism: reproductive tracts and mammogenesis. ~~Consequently, CaV3.1 is highlighted as a potential pharmacological target to modulate differential sexual developmental of fat deposition and mammogenesis~~.

Introduction

Obesity and its clinical management is a worldwide problem. Obesity is associated with increase in morbidity and mortality rates through predominantly cardiovascular and metabolic dysfunction, as well as an increased risk of cancer. In particular it well established that obesity is associated with both an increased risk of post-menopausal breast cancer as well at its reoccurrence, where weight loss reduces this risk (Jiralerspong & Goodwin, 2016; Kothari *et al.*, 2020). White fat adipose (WFA) is a major component of mammary gland tissue and undergoes various morphological and functional changes with puberty, pregnancy, lactation, involution, and menopause (Kothari *et al.*, 2020; Colleluori *et al.*, 2021). Indeed, the intimate relationships between WFA and mammary gland function is suggested as an ideal microenvironment for the initiation and maintenance of breast cancer (Kothari *et al.*, 2020; Colleluori *et al.*, 2021).

Obesity is due to increased ~~white fat adipose (~~WFA~~)~~ mass through hypertrophy and hyperplasia of white fat adipocytes. Adipocytes primarily act as an energy reservoir to store excess energy as triglycerides via lipogenesis during times of excess and release energy, as lipids via lipolysis, in time of demand (Arner *et al.*, 2011). Since many functions of

WFA are regulated by Ca^{2+} this makes Ca^{2+} metabolism a potential therapeutic target to regulate obesity (Fedorenko *et al.*, 2020). For example, lipolysis in WAT is promoted by extracellular Ca^{2+} influx though voltage-gated calcium channels (CaVs) (Izawa *et al.*, 1983; Fedorenko *et al.*, 2020; Akaniro-Ejim & Smith, 2021). ~~although it is unclear if CaV-mediated Ca^{2+} influx is also necessary for insulin-sensitive glucose uptake and lipogenesis (Draznin *et al.*, 1987; Avasthy *et al.*, 1988; Fedorenko *et al.*, 2020).~~ CaV-mediated Ca^{2+} influx also helps explain why changes in extracellular Ca^{2+} can modulate proliferation, differentiation and expansion of adipocytes; processes that underlie the hypertrophy and hyperplasia of adipose tissue associated with obesity (Oguri *et al.*, 2010; Sun *et al.*, 2012; Zhang *et al.*, 2018) although the mechanisms are unknown. Interestingly, these processes are differentially regulated between males and females (Demerath *et al.*, 2007; Chang *et al.*, 2018; Schorr *et al.*, 2018).

Consequently, given the multiple effects of CaVs activity in WAT, CaVs may be a novel target to effect fat disposition; a notion already supported by the ability of CaV antagonists to decrease FFA levels in-vivo (Hvarfner *et al.*, 1988; Cignarella, 1994) as well as impede weight gain in mice (Uebele *et al.*, 2009).

The properties of CaVs are extensively documented (Catterall, 2011; Zamponi *et al.*, 2015). CaVs are heteromeric structures organised around a membrane-intrinsic $alpha_1$-subunit; $alpha_1$. $alpha_1$ forms the ion–channel pore, imparts voltage sensitivity and supports drug binding

(Zamponi *et al.*, 2015). ~~In addition,~~Whereas the intracellular accessory subunits: beta-, gamma- and alpha$_2$- delta are membrane-extrinsic proteins that modify alpha$_1$-subunit expression and function (Dolphin, 2016). The CaV alpha$_1$-subunit is encoded by 10 genes which are grouped into 3 classes: L-type, CaV1.1-CaV1.4; P, Q and N-type, CaV2.1-2.3; T-type, CaV3.1-3.3. Each class has its own unique properties of voltage-sensitivity, inactivation, biophysics, pharmacology and regulation; properties further diversified by tissue-dependent splice variation, phosphorylation and subunit combination (Catterall, 2011; Zamponi *et al.*, 2015; Dolphin, 2016).

Previous work from our laboratory has demonstrated mRNA transcripts and protein expression of the alpha$_1$ subunit for L-type CaVs, CaV1.2 (*Cacna1c*) and CaV1.3 (*Cacna1d*), as well their accessory subunits, in adipocytes isolated from rat epididymal fat pads (Fedorenko *et al.*, 2020). Mainly because of size and accessibly, epididymal fat ~~pads are an~~is the foremost ~~-~~established model to explore visceral WAT physiology (Chusyd *et al.*, 2016). However, other visceral as well as subcutaneous fat depots are recognised in the aetiology of metabolic disease, a condition that arises through depot-dependent differences in adipokine secretion, lipogenesis, lipolysis and adipocyte remodelling (Arner *et al.*, 2011; Chusyd *et al.*, 2016). Moreover, epididymal fat is exclusively male in origin, but since the aetiology of human metabolic disorders ~~is influenced by sex~~ and that fat pad patterning itself ~~is~~ are sex dependent (Chusyd *et al.*, 2016; Valencak *et al.*, 2017)~~,~~ necessitates an exploration of sexual

dimorphism in WAT physiology and CaV expression. For example, ~~In~~ in heart ~~for example~~ CaV expression changes with puberty and sexual maturation (Sims *et al.*, 2008). To date, the expression profile of CaVs in murine WAT depots and how these vary with sex and puberty are unknown. Although electrophysiological approaches provides unequivocal functional characterisation of CaVs, its application to primary fat cells is technically difficult (Bentley *et al.*, 2014; Fedorenko *et al.*, 2020; Akaniro-Ejim & Smith, 2021). Secondly, given the common mesenchymal origin of ~~, as well as metabolic interplay between,~~ different fat depots, any attempt~~s~~ to modify the function and development of a specific fat depot via conditional transgenic knockout ~~are also~~becomes problematic. Thirdly, transgenics approaches are confounded by compensatory mechanisms known to occur for these channel types (Namkung *et al.*, 2001; Uebele *et al.*, 2009; Wang *et al.*, 2016). Consequently, we have used a transcriptomics ~~snapshot~~ as a pragmatic method to ~~screen~~ explore CaV expression ~~diverse WAT sources for CaV expression for a given sex and time~~.

Our primary aim was to use molecular biological approaches to explore how the normative expression levels of CaVs vary with depot, age, and age in WAT deposits from rats under fed ad-libitum conditions. The secondary aim was to determine if CaV activity affects adipogenesis in pre adipocyte cell model.

Commented [PS1]: Model for man

Materials and methods

137 Isolation and preparation of adipocytes

138 Animal care and experimental procedures were locally approved (ASPA
139 000187, University of Nottingham) and performed in accordance with the
140 UK Home Office Animals (Scientific Procedures) Act (1986). Animals were
141 obtained from Charles River (RRID:RGD_2308816), kept group housed
142 with a 12-hour light dark cycle and fed ad libitum. Animals were killed by
143 cervical dislocation. Fat depots were excised from pre-eostropausal adult
144 (P270>P>140; 280 – 300g) and juvenile (P14-30) Wistar rats. For
145 subcutaneous fat, we used inguinal depots (IWAT) and for visceral:
146 retroperitoneal, mesenteric, and gonadal: epididymal from males and
147 periovarian from females. Primary white fat adipocytes were prepared
148 from depot explants as previously described (Bentley *et al.*, 2014).
149 Dissection and isolation of adipocytes was performed in a Hank's buffer
150 solution supplemented with 5 mM glucose and 0.5% wt/vol BSA (Sigma
151 A3058). After excision, depots were washed in Hanks and visible blood
152 vessels expurgated. Depots were cut into ~ 5 mm pieces and added to a
153 25 ml Nalgene *Erlenmeyer* flask which contained 6 mls of Hanks with 1mg
154 ml^{-1} Type II collagenase (Sigma C6885) and minced for 1 minute.
155 Adipocytes were liberated by a 30-50 minute collagenase digestion with
156 mild agitation at 37^{o}C. Digestion progress was indicated by the
157 appearance of the buoyant band of adipocytes. Digestion was halted by
158 dilution and cooling via the addition of 20 ml of Hanks' at 20-22^{o}C. The
159 digest was then filtered through a 250 μM nylon mesh (Normesh limited,
160 Oldham, UK) and the filtrate collected in an inverted 50ml syringe.

Adipocytes separated from the buffer by flotation to form a buoyant layer whereas cell debris and other cell types precipitated out. After 5 minutes the infranatent and cell debris were removed and the process of separation by flotation repeated twice more by further additions of 20 ml of buffer and subsequent drainage. After the final drain, the adipocytes were suspended in 2 ml Hank's solution, spun down at 1,000 g for 10 minutes to obtain packed cells for subsequent molecular biology.

Differentiated 3T3-L1 cells, an established model of mouse IWAT were also prepared and validated as detailed elsewhere (Bentley *et al.*, 2014). Briefly, 3T3-L1 pre-adipocytes (passage number less than 17) were differentiated into adipocytes by exposure to DMEM media plus 10% foetal bovine serum (FBS) supplemented with 1 µg/ml insulin, 0.5 mM IBMX, 0.25 µM dexamethasone and 2 µM rosiglitazone and subsequently maintained in DMEM plus 10% FBS alone. Differentiation was confirmed by Oil red O staining. Experiments were carried out on day 8.

RNA Extraction

Total RNA was extracted from either freshly isolated adipocytes, or those previously frozen at -80ºC. This was performed with a RNAesy Lipid Tissue kit, which included QIAzol Lysis Reagent, in accord with the manufacturer's instructions (Qiagen).

RNA sequencing

RNA quantity was determined with the Qubit RNA BR Assay Kit and Qubit Fluorometer (Thermo Fisher, RRID: SCR_018095). RNA integrity was

assessed with the Agilent TapeStation 4200 and Agilent RNA ScreenTape Assay Kit (Agilent). mRNA was then purified from 1 μg of total RNA with the NEBNext Poly(A) mRNA Magnetic Isolation Module (E7490, New England Biolabs). Indexed sequencing libraries were prepared with the NEBNext Ultra II Directional RNA Library Preparation Kit for Illumina (New England Biolabs) and NEBNext Multiplex Oligos for Illumina (96 Unique Dual Index Primer Pairs, New England Biolabs). Constructed Libraries were quantified using the Qubit Fluorimeter (ThermoFisher Scientific, RRID:SCR_018095) and the Qubit dsDNA HS Kit (ThermoFisher Scientific) and their fragment-length distributions analysed with the Agilent TapeStation 4200 and the Agilent High Sensitivity D1000 ScreenTape Assay (Agilent). The libraries were then pooled in equimolar amounts and a final library quantification performed using the KAPA Library Quantification Kit for Illumina (Roche). The library pool was sequenced on an Illumina NextSeq 500 (RRID: SCR_014983; Illumina), to generate over 100 million pairs of 75-bp paired-end reads per sample. Trimming and analysis of obtained data were performed with Galaxy (RRID:SCR_006281) and Integrated Genome Viewer software (RRID:SCR_011793).

The homogeneity and purity of our isolated adipocyte preparations were confirmed by the absence of RNA for the specific markers of other cell types present in WAT: Sympathetic neurons, Synaptic Vesicle Monoamine Transporter (VMAT), neuronal Nuclei antigen (NeuN); Parasympathetic Neurons; Choline O-Acetyltransferase (Chat), neuronal Nuclei antigen

(NeuN); Astrocytes, Glial Fibrillary Acidic Protein (GFAP); Endothelia, Endothelial cell adhesion molecule-1 (CD31); Smooth Muscle, Smooth Muscle Protein 22-Alpha (SM22) and the L-type voltage-gated calcium channel alpha$_1$S subunit (CaV1.1, Cacna1s); and for macrophages Transmembrane Immune Signalling Adaptor (Tyrobp), and Adhesion G Protein-Coupled Receptor E1 (Adgre1). In the RNA-seqs, FPKM for all markers but macrophage were zero; with geometric mean FPKMs of 14 and 1.2 for Tyrobp and Adgre1 respectively: data indicative of macrophage contamination (Ying *et al.*, 2017). Reads of specific markers of white fat adipocytes: adiponectin (ADIPOQ), leptin (LEP) and S100 calcium-binding protein B (S100B), had respective geometric mean FPKMs of 1415, 421 and 540.

Quantitative Polymerase Chain reaction

The concentration of isolated RNA was determined with a NanoDrop Spectrophotometer (Thermofisher) and its quality checked via an Aligent bioanalyzer (Aligent). RNA samples were treated with DNase I (Thermofisher) to remove genomic DNA, and cDNA synthesis was performed using 1 µg of total RNA with SuperScript™ III Reverse Transcriptase (10 units / µl RNA, Thermofisher).

Standard PCR reactions were performed in a total volume of 25 µl using DreamTaq PCR MasterMix (Thermofisher), with 2 µl of cDNA product (from a 20 µl RT reaction) and 1.25 µM of each specific primer pair (Table 1). PCR was performed at 95°C for 10 min, followed by 95°C for 15 sec

then 40 cycles at the specific primer annealing temperature, and 72°C for 35 secn. The last cycle was followed by a final extension step at 72°C for 10 min. PCR products were size fractionated on 1% (w/v) agarose gels stained with SYBR™safe (Thermofisher) and imaged under UV light with GeneSnap software (Syngene, UK).

Generated cDNAs were sequenced to identify the PCR product which confirmed the sequence of the channel type.

Quantitative polymerase chain reaction (qPCRs) was used to determine gene expression level. qPCRs were performed in triplicate with SYBR® Green JumpStart TM Taq ReadyMix™ (Sigma) master mix, and detection was performed using the Rotor-Gene 6000 cycler (Corbett Research). qPCR was performed at 95°C for 10 minutes, followed by 40 cycles of denaturation at 95ºC for 15 seconds, 30 sec at the specific primer annealing temperature, and elongation at 72ºC for 40 seconds. For reference, three housekeeping genes were used: TATA-box, GAPDH and PGK-1.

The resultant mean threshold cycle (Ct) values were used for reference gene normalisation and gene expression analyses. Relative quantification was performed by the method of Pfaffl (Pfaffl, 2001).

Effect of CaV blockers on adipogenesis

TTA-A2, IC_{50} ~5 µM (Kraus *et al.*, 2010) and Calciseptine IC_{50} ~10 nM (De Weille *et al.*, 1991) selective blockers of CaV3.x and CaV1.x respectively, as well as mibefradil which has 12-13 greater potency on CaV3.x, IC_{50} ~1 µM than CaV1.x (Martin *et al.*, 2000) (Alomone, Israel), were freshly applied to 3T3-L1 cells prior to and post differentiation with each media exchange. On the eighth day, cell proliferation was determined by nuclear density and differentiation by lipid content. Nuclei were stained with Hoechst 33342 (ThermoFisher) at 10µg ml^{-1} in Hanks for 30 minutes. After twice washing in PBS, lipid was stained by 10µg ml^{-1} Nile Red (NR) (ThermoFisher) in Hank's for 10 minutes. Dye content was detected with a SpectraMax M2 microplate spectrophotometer (Molecular Devices, USA) with 350 nm excitation/490 nm emission for Hoechst 33342 and 510 nm excitation/590 nm emission for NR. After background correction, the NR to Hoechst fluorescence ratio was taken as an index of adipogenesis~~.~~. Overlayed images were captured with a Zeiss ERc 5rs Axiocam attached to an ZeissAxio with a 20x objective and filter sets at indicated above. Images were acquired with Zeiss Zen software and analysed with Digimizer (MedCalc Software Ltd)

Statistical analysis

Statistical analyses were performed using Graphpad PRISM Ver. 9.4 (RRID: SCR_002798). Distributions were checked for normality with the D'Agostino & Pearson omnibus test. Inferential tests are given in the text.

Data are shown as scatter plots ~~overlaid~~ with the mean ± S.D or as box plots with the median, 25%-75% interquartile and 5%-95% ranges. ~~Numerical d~~Data are given as mean± S.D or median with 5 to 95% confidence intervals (95% C.I.) to 3 significant figures, where n is the number of different animal preparations. Unless stated otherwise statistically significance was assigned when $p < 0.05$ and in graphics is flagged as *, ** when $P < 0.01$, *** when $P < 0.001$ and **** when $P < 0.0001$.

Results

qPCR (Figs 1A, B) confirmed CaV1.2 (*Cacna1c*) as the predominant CaV expressed in rat epididymal and subcutaneous adipocytes; followed by *CaV1.3 (Cacna1d)* and then *CaV2.1 (Cacna1a), CaV2.3 (Cacna1e),* CaV3.1 (*Cacna1g*), CaV3.2 (*Cacna1h*) and CaV3.3 (*Cacna1i*) at similar amounts, with little to no expression of CaV1.1 (*Cacna1s*), CaV1.4 (*Cacna1f*), or CaV2.3 (*Cacna1b*). qPCR integrity was confirmed by the generation of a correlation matrix for the relationships between the 13 rat qPCr CaV expression profiles; this showed that the profiles were significantly similar for all animals (Fig. ~~1E~~1C). The RNA-seq transcriptome of epididymal adipocytes (Fig. ~~1C~~1D) reports a slightly different expression profile to qPCR with CaV3.1 (*Cacna1g*) and CaV3.2 (*Cacna1h*) expressed to a similar level as CaV1.2 (*Cacna1c*). The expression levels of the CaV transcripts from the RNA-seq FPKM data were, however, well correlated (R=0.6, P=0.0002; Pearson) with those from qPCR (Fig. 1F). Figure ~~1D~~ 1E shows that rat epididymal adipocytes express all known $\alpha_2\delta$ and β accessory subunits, but only *Cacng*4 and *Cacng*7 ϒ subunits.

Given the relevance of the L-type CaV1.2 and CaV1.3, to adipocyte function (Fedorenko *et al.*, 2020) and that of T-type CaV3.1 to adipocyte development (Uebele *et al.*, 2009; Oguri *et al.*, 2010) we specifically

investigated the distribution of these three CaV isoforms in other fat depots and explored how these varied with age and sex.

Figure 2 illustrates that there were no significant differences in the levels of transcript for *Cacna1c*, *Cacna1d Cacna1g, Cacna1h* or *Cacna1i* (One Way ANOVA, Kruskal Wallis) between gonadal, retroperitoneal, mesenteric and IWAT within a given sex for adults (Figs. 2A-E). Figure 2F compares the expression levels of all five genes subsequently pooled from the different depots from adults for either sex. In adults, the expression levels of *Cacna1c, Cacna1d, Cacna1h and Cacna1i* also did not differ between sexes (Figs. 2A-B, D-E), however, the expression of *Cacna1g* (CaV3.1) was significantly greater in female adults than in males for gonadal, mesenteric and IWAT, but not retroperitoneal depots (Fig. 2C; One Way ANOVA). A different picture for gene expression was observed in juvenile rats (p15-30) (Figs. 2G-I), where with the exception for *Cacna1c* in juvenile retroperitoneal, there was no significant difference (One way ANOVA) in the expression of *Cacna1c*, *Cacna1d* or *Cacna1g* between either depot or sex.

Figure 3 show the expression levels of *Cacna1c*, *Cacna1d* and *Cacna1g* compared within a depot type. The rank order of expression for juveniles of both sexes, other than for male juvenile mesenteric, were the same: CaV1.2>CaV1.3>CaV3.1 (CaV3.2 and CaV3.3 not detected). For male adults the rank order of CaV gene expression was CaV1.2>CaV1.3>CaV3.1>CaV3.2=CaV3.3 whereas in female adult the rank order of CaV gene expression was different:

CaV1.2>=CaV3.1>1.3>CaV3.2=CaV3.3; a variation due to the heightened expression of CaV3.1 (*Cacna1g*) seen in females.

Since the relative expression for *Cacna1c*, *1d* and *1g* in adult animals (Figs. 2A, B, C) appeared to be smaller than that found in juveniles' (Figs. 2G, H, I) we explored the effect of age on gene expression. Figure 4 shows that the expression of *Cacna1c* (CaV1.2) differentially changed with sex post puberty, with decreases seen in gonadal, retroperitoneal and IWAT depots for females (Fig. 4A, D, J), whereas for males a decrease was only seen in gonadal depots (Fig. 4A). *Cacna1d* (CaV1.3) also changed expression with age, but this phenomenon was dependent on depot and independent of sex; with decreases seen in gonadal and mesenteric depots for both males and females (Fig. 4B, H). As for *Cacna1g* (CaV3.1), its expression decreased with age only in male gonadal and IWAT depots (Figs. 4C, L) whereas for females it remained unchanged in gonadal depots and increased ~ 2 fold in IWAT (Figs 4C, L). In summary, for most tissues in both sexes all three CaVs isoforms either did not change expression or were down regulated post puberty, except for *Cacna1g* (CaV3.1) in inguinal (mammary) depots in females which increased. The coefficient of variation decreased by ,14±18% ($p<0.001$ Paired t-test) with post puberty; data indicative of greater transcript variation in the juvenile depots.

Formatted: Font: 12 pt, Font color: Black

A commonly used adipocyte cell-line model is differentiated 3T3-L1 (mouse fibroblast) cells (Oguri *et al.*, 2010; Bentley *et al.*, 2014). We compared the gene expression for *Cacna1c*, *Cacna1d* and *Cacna1g* in

355 undifferentiated and differentiated 3T3-L1 cell lines (Fig. 5A-C). *Cacna1c*
356 (CaV1.2) and *Cacna1g* (CaV3.1) had significantly greater expression in
357 undifferentiated 3T3-L1 pre-adipocytes than when differentiated into
358 adipocytes (Figs. 5A, C). *Cacna1d* (CaV1.3) expression did not differ
359 between differentiated and differentiated 3T3-L1 cells (Fig. 5B).

360 Give the putative role of CaV3.1 in adipocyte development (Uebele *et al.*,
361 2009; Oguri *et al.*, 2010) we investigated the effect of the selective
362 blockers of this channel: mibefradil and TTA-A2 on preadipocyte
363 proliferation and differentiation. Both mibefradil and TTA-A2 at their
364 respective IC_{50} values promoted proliferation, as revealed by Hoechst
365 staining (Figs. 7A, 7B). However, although the ability of the cell
366 population to differentiate and store lipid as indicated by their ability to
367 accumulate Nile red was like control cells (Figs. 6, 7B, 7E), the fact the
368 cells were almost twice as dense than control suggest differentiation was
369 impaired; an idea supported by the significant decrease in the Nile
370 red/Hoechst ratios (Figs. 6, 7C, 7F). Calciseptine, a selective peptide
371 inhibitor of CaV1.x was without effect on either proliferation or
372 differentiation (Figs. 6, 7G-I).

373 **Discussion**

374 Consistent with our previous work (Fedorenko *et al.*, 2020) we found the
375 predominant voltage-gated calcium channels genes expressed in rat
376 epididymal fat are *Cacna1c* (CaV1.2), *Cacna1d* (CaV1.3) and *Cacna1g*
377 (CaV3.1). We now show that ~~the levels of~~ CaV1.2 and CaV1.3 gene
378 expression do<u>es</u> not differ across gonadal, retroperitoneal, mesenteric,

and inguinal subcutaneous (IWAT) fat depots for juvenile or adult rats of either sex. Moreover, except for CaV1.2 in juvenile retroperitoneal fat, no difference between sexes was observed for the expression levels for CaV1.2 and CaV1.3 for either juvenile or adult animals. In contrast, in adults, but not juveniles, CaV3.1 had a greater expression in adipocytes from gonadal, mesenteric and IWAT, depots from female compared to male. Although within a given sex CaV3.1 expression did not alter with puberty in either retroperitoneal or mesenteric depots, it did decrease in male epididymal gonadal and IWAT fat depots. Whereas in females, CaV3.1 did not change in periovarian gonadal depots but increased with puberty in IWAT depots.

We occasionally found transcripts for CaV3.2, as well as CaV3.3 in some adult samples, although these were scarce and often undetectable. Published RNA-seq from differentiated 3T3-L1s do not demonstrate transcripts of CaV3.2 and CaV3.3 (Zhang *et al.*, 2017) which throw doubt on an adipocyte origin for these two transcripts. Transcripts for CaV3.2 and CaV3.3, but not CaV3.1, have been identified in macrophages, a cell type which contaminates our adipocyte preparations as indicated by the presence of their specific marker genes: Tyrobp and Adgre1 (Ying *et al.*, 2017). Indeed, transcriptomes of human and mouse immune t-cells show CaV2.1, CaV3.2 and CaV3.3 in human and CaV2.1 and CaV3.2 in mouse with little evidence of CaV3.1 (Erdogmus *et al.*, 2022). The Immunological Genome Project (Heng *et al.*, 2008) similarly supports these findings with the majority of immune b-cell and macrophage CaV3.x transcripts

encoded by CaV3.2 (Cacna1h) and CaV3.3 (Cacna1i), with little expression of CaV3.1 (Cacna1g). The absence of CaV1.2 and CaV1.3 transcripts in macrophages suggest that the changes observed in the present study are solely attributed to white fat adipocytes (Heng *et al.*, 2008; Erdogmus *et al.*, 2022).

Our data suggest that CaV3.1 may have a crucial role in female adult adipose tissue that relates to sexual dimorphism in fat deposition and function (Newell-Fugate, 2017). CaV3.1 is established to be upregulated in the hypothalamus and pituitary of rodents by a process that involves oestrogen (Qiu *et al.*, 2006; Zhang *et al.*, 2009) however the signalling cascade has yet to identified.

With the onset of puberty a twofold increase in serum oestradiol (E2) ensues in female (P30-P40 rats) (Parker & Mahesh, 1976) but not male rats (Bell, 2018). The actions of oestrogens in adipose are depot dependent: decreasing visceral but not subcutaneous adiposity (Cooke *et al.*, 2001; D'Eon *et al.*, 2005; Bjune *et al.*, 2022); ideas supported by the observation that global nuclear oestrogen receptor ESR1 (ERα) knockout animals become susceptible to obesity via visceral fat gain (Cooke *et al.*, 2001; Foryst-ludwig *et al.*, 2008; Winn *et al.*, 2023); a finding consistent with humans where ESR1 expression transcript is negatively correlated with female waist to hip ratio indicative of subcutaneous weight gain (Ahmed *et al.*, 2022). With regard to sexual dimorphism, ESR1 protein expression is found to be larger in inguinal (mammary) subcutaneous adipose from post-pubescent female mice and pigs compared to their age

matched male counterparts (Winn *et al.*, 2023); data that mirrors our Cacna1g transcript expression profile we found for adult rats. This finding supports the idea that oestrogen may promote/maintain Cacna1g transcription in adipocytes, like that established in rodent brain (Qiu *et al.*, 2006; Zhang *et al.*, 2009), or alternatively, ESR1 and Cacna1g are permissive partners for inguinal fat development.

Given the permissive role extracellular Ca^{2+} influx plays in sympathetic mediated lipolysis (Izawa *et al.*, 1983), an increased expression of CaV3.1 in post-pubescent female fat tissue may enhance this process like that already observed when CaV1.x activity is augmented by dihydropyridine agonists (Fedorenko *et al.*, 2020).

In an additional study (Supplementary Figure 1), we observe no difference in basal $[Ca^{2+}]_i$ nor cell diameter in adipocytes isolated from male and female adult mouse IWAT; data that suggests that CaV3.1, neither controls basal $[Ca^{2+}]_I$ adipocyte or size, but more likely is involved in the processes of differentiation and hyperplasic, but not hypertrophic, adipogenesis~~Increased expression of CaV3.1 may control Ca^{2+} influx necessary for adipocyte development~~ as previously observed (Uebele *et al.*, 2009; Oguri *et al.*, 2010) and we now show. The decrease in the coefficient of variation post puberty suggest that the pre-pubescent tissue contains a range of developmental states that is lost on adulthood, something that is not observed using the cell line.

Since adipogenic oestrogen, is critical to the development of the murine female reproductive system and function (Wang *et al.*, 2017), the

increased CaV3.1 expression we detect in murine ovarian fat may well relate to adipogenesis and its subsequent provision of a suitable paracrine interactions to develop and maintain the rodent female reproductive tract (Reverchon *et al.*, 2014).–WFA have a key role in the synthesis and storage of oestrogens. In particular they express aromatase which catalyses the conversion of adrenal androgens, such as testosterone and androstenedione, to the aromatic oestrogens (estradiol-E2 and estrone-E1) (Mair *et al.*, 2020). Indeed removal of periovarian fat in mice leads to a several fold decrease in circulating oestrogen levels, irregular oestrus, impaired folliculogenesis and infertility (Wang et al., 2017) However, since humans do not appear to have gonadal fat (Chusyd *et al.*, 2016; Börgeson *et al.*, 2022) these conclusions do not translate to man. Importantly, murine IWAT does contain the 4th and 5th mammary glands (Grove *et al.*, 2010; Chusyd *et al.*, 2016) with WFA established to be critical in mammary ductal formation and functional plasticity for both mouse and man (Kothari *et al.*, 2020; Colleluori *et al.*, 2021). Consequently, the CaV3.1 expression profiles changes we observed in IWAT may relate to the established association between the paracrine action of adipocytes and human mammogenesis (Colleluori *et al.*, 2021)~~, a secondary sexual characteristic regulated by oestrogen~~.

Connected with this observation is the fact that CaV3.1 blockers such as pimozide and mibefradil are shown to be antiproliferative in adipose models of breast cancer (Bertolesi *et al.*, 2002), an observation we now confirm for 3T3-L1 adipogenesis. Indeed, antagonists of T-type VGCCs

475 are proposed to be a potential treatment for breast cancer (Bhargava &
476 Saha, 2019). The abilities of in-vivo administration of TTA-A2, a CaV3.1
477 selective antagonist, as well as that of genetic knockout of *Cacna1g*
478 (CaV3.1) to both inhibit of high-fat weight gain in mice (Uebele *et al.*,
479 2009), emphasize the importance of CaV3.1 in adipogenesis; our
480 observations with the ability of TT-A2 and mibefradil, selective blockers of
481 CaV3.1, but not that of CaV1.x: calciseptine, to inhibit adipogenesis of
482 3T3-L1 cells is consistent with this idea. It must be noted however that
483 data obtained with genetic knockouts of CaV3.1 may be muted through
484 compensatory expression of other CaVs like that already observed with
485 macrophages (Wang et al., 2016). At 10μM, mibefradil can mobilise
486 intracellular Ca^{2+} stores (Souza Bomfim *et al.*, 2021), so interpretation of
487 its effects should be treated with caution.

488 3T3-L1 cells are widely used for studies of adipocyte differentiation.
489 Unlike primary adipocytes, gene expression in undifferentiated 3T3-L1
490 pre-adipocytes was similar for all three channel isoforms: CaV3.1 ~
491 CaV1.2 ~ CaV1.3; where the CaV3.1 and CaV1.2, transcript levels
492 decreased with differentiation; an observation like that we observed in all
493 our post-pubescent rat fat depots apart from CaV3.1 in female depots
494 associated with secondary sexual characteristics. Our results for CaV3.1
495 expression in 3T3-L1 cells confirm those previously reported in this cell
496 line (Uebele *et al.*, 2009; Oguri *et al.*, 2010). The decrease in CaV3.1
497 expression we observed after differentiation may be associated with a
498 subsequent redundancy of functional protein; results already observed

with the loss of CaV3.1 protein in Western blots with 3T3-L1 on differentiation (Oguri *et al.*, 2010). Although, our data support the involvement of CaV3.1 in the differentiation of pre-adipocytes into mature adipocytes, however we draw the contrary conclusion to others (Oguri *et al.*, 2010) in regard to its role in proliferation since we observed that its pharmaceutical inhibition augmented proliferation. A difference possibly explained by our use of a longer, 10 day compared to 24 hr incubation in drug (Oguri *et al.*, 2010), a procedure necessary to encompass the cell cycle length of 30-40 hrs.

With regard to the sex dependent differences we observed for CaV expression, this may be a case of differential gene regulation by gonadal hormones such as oestrogen (D'Eon *et al.*, 2005; Qiu *et al.*, 2006) or alternatively it may relate to the autosomal genome (Newell-Fugate, 2017; Chang *et al.*, 2018); indeed over 100 genes are differentially expressed in WAT that are independent of gonadal hormones as demonstrated by studies in ovariectomized mice, however none of the genes within that study were CaVs (Grove *et al.*, 2010). Of the genes that are suggested to be sexually dimorphic in WAT, several were reputed to be CaVs: *Cacna1s, Cacna1f and Cacna1e* (GEO ascension GSE3086) (Yang *et al.*, 2006). However, none of these genes were identified to be sexually dimorphic in our present study. An important difference between this previous study (Yang *et al.*, 2006) and ours is that we used purified isolated adipocytes whereas the former used whole adipose tissue; for whom the transcriptome is for a population of different cell types; this

explains why Yang (Yang *et al.*, 2006) observed expression of *Cacna1s* (CaV1.1) a marker gene for smooth muscle; a gene we did not detect in our purified samples.

To consolidate these ideas, additional RNA-seq revealed expression of the membrane g-protein coupled oestrogen receptor gene transcript, GEPR1 (GRP30), and the nuclear oestrogen receptor ESR1 (ERα) , of these ESR1 had the greatest expression, a transcript not found in immune cells and so is likely to arise solely from adipocytes. In gonadal fat from three male rats ESR1 and GPER1 were expressed with median FPKMs of 15.3 and 0.37 respectively; data which supports the existence of an oestrogenic sensitive signal cascades in primary white fat adipocytes.

Genes like *Cacna1g* (CaV3.1) and *Cacna1c* (CaV1.2) are sexually dimorphic at both the transcriptomic and functional level in murine tissues such as brain (Qiu *et al.*, 2006; Zhang *et al.*, 2009) and heart (Sims *et al.*, 2008), and as we now report, in white fat adipocytes too. Interestingly in man, a single nucleotide polymorphism is reported near the CACNA1D (CaV1.3) locus that is associated with a significant increase in human abdominal to subcutaneous adipose tissue ratio (Sung *et al.*, 2016); data that further support a role for CaVs in fat deposition.

Physiological relevance.

Mature primary adipocytes and differentiated 3T3-L1s have a plasma membrane potential of -30 mV that ranges between -15 to -50 mV (Bentley *et al.*, 2014). These voltages are sufficiently depolarised to

constitutively activate both CaV1.2 and Ca1.3 to elicit a sustained window Ca^{2+} influx into these cells (Crunelli *et al.*, 2005; Fedorenko *et al.*, 2020; Akaniro-Ejim & Smith, 2021). Although, at these ~~adipocyte~~ membrane potentials CaV1.2, but not CaV1.3, is expected to undergo voltage-dependent inactivation ~~is sufficiently depolarised to activate CaV3.1, it is also predicted to completely inactivate the channel to render it closed and impermeable to Ca^{2+} influx , however~~ this probably does not occur in ~~adipocytes in situ~~ since in adipocytes ~~the~~ its voltage-dependence ~~of CaV3.1 inactivation~~ is sufficiently shallow to prevent complete inactivation (Oguri *et al.*, 2010) and ~~to~~ permit a constitutive Ca^{2+} influx ~~window~~ (Crunelli *et al.*, 2005) and consequently a sensitivity to CaV1.2 blockers as observed in this study. Since adipocytes are electrically inactive, Ca^{2+} influx is not modulated by changes in membrane potential but by other means; for example growth hormone activates CaV1.2/3 and promotes Ca^{2+} influx in mouse primary adipocytes (Akaniro-Ejim & Smith, 2021). Our present data suggests that CaV3.1 maybe modulated by gene expression, possibly via oestrogen as seen in neuronal tissues (Qiu *et al.*, 2006; Newell-Fugate, 2017).

Taken together, our data suggests that the elevated expression of CaV3.1 in females is not involved global adipogenesis but directed in depots that have a dynamic growth profile such as murine and human mammary glands where changes occur with pregnancy, lactation and involution as well as oestrus in murines. The fact that CaV3.1 is an established clinical drug target to treat human breast cancer and that CaV3.1 antagonists

inhibit weight gain in mice suggest that modulation of this CaV may be beneficial in the control of secondary sexual characterstic functions~~adiposity and its associated consequences~~.

Acknowledgements

This work was supported by the Leverhulme Trust (Grant ID: RPG-2017-162).

Conflict of interest

The authors declare that they have no conflict of interest.

References

Ahmed F, Kamble PG, Hetty S, Fanni G, Vranic M, Sarsenbayeva A, Kristófi R, Almby K, Svensson MK, Pereira MJ & Eriksson JW (2022). Role of Estrogen and Its Receptors in Adipose Tissue Glucose Metabolism in Pre- and Postmenopausal Women. *J Clin Endocrinol Metab* **107,** 1879–1889.

Akaniro-Ejim NE & Smith PA (2021). Intracellular Ca2+ in Mouse White Fat Adipocytes: Effects of Extracellular Anions, Growth Hormone, and Their Interaction with Ca2+ Influx. *Bioelectricity* **3,** 282–291.

Arner P, Bernard S, Salehpour M, Possnert G, Liebl J, Steier P, Buchholz BA, Eriksson M, Arner E, Hauner H, Skurk T, Rydén M, Frayn KN & Spalding KL (2011). Dynamics of human adipose lipid turnover in health and metabolic disease. *Nature* **478,** 110–113.

Bell MR (2018). Comparing postnatal development of gonadal hormones and associated social behaviors in rats, mice, and humans. *Endocrinology* **159,** 2596–2613.

Bentley DC, Pulbutr P, Chan S & Smith PA (2014). Etiology of the membrane potential of rat white fat adipocytes. *Am J Physiol - Endocrinol Metab* **307,** E161–E175.

Bertolesi GE, Shi C, Elbaum L, Jollimore C, Rozenberg G, Barnes S & Kelly MEM (2002). The Ca2+ channel antagonists mibefradil and pimozide

inhibit cell growth via different cytotoxic mechanisms. *Mol Pharmacol* **62,** 210–219.

Bhargava A & Saha S (2019). T-Type voltage gated calcium channels: a target in breast cancer? *Breast Cancer Res Treat* **173,** 11–21.

Bjune J, Strømland PP & Jersin RÅ (2022). Metabolic and Epigenetic Regulation by Estrogen in Adipocytes. *Front Endocrinol (Lausanne)* **13,** 1–11.

Börgeson E, Boucher J & Hagberg CE (2022). Of mice and men: Pinpointing species differences in adipose tissue biology. *Front Cell Dev Biol* **10,** 1–8.

Catterall WA (2011). Voltage-Gated Calcium Channels. *Cold Spring Harb Perspect Biol* **3,** a003947.

Chang E, Varghese M & Singer K (2018). Gender and Sex Differences in Adipose Tissue. *Curr Diab Rep*; DOI: 10.1007/s11892-018-1031-3.

Chusyd DE, Wang D, Huffman DM & Nagy TR (2016). Relationships between Rodent White Adipose Fat Pads and Human White Adipose Fat Depots. *Front Nutr*; DOI: 10.3389/fnut.2016.00010.

Cignarella A (1994). Antithrombotic activity of nicardipine in spontaneously hypertensive rats. *Pharmacol Res* **30,** 273–280.

Colleluori G, Perugini J, Barbatelli G & Cinti S (2021). Mammary gland adipocytes in lactation cycle, obesity and breast cancer. *Rev Endocr Metab Disord* **22,** 241–255.

622 Cooke PS, Heine PA, Taylor JA & Lubahn DB (2001). The role of estrogen
623 and estrogen receptor- a in male adipose tissue. *Mol Cell Endocrinol*
624 **178,** 147–154.

625 Crunelli V, Tóth TI, Cope DW, Blethyn K & Hughes SW (2005). The
626 "window" T-type calcium current in brain dynamics of different
627 behavioural states. *J Physiol* **562,** 121–129.

628 D'Eon TM, Souza SC, Aronovitz M, Obin MS, Fried SK & Greenberg AS
629 (2005). Estrogen regulation of adiposity and fuel partitioning:
630 Evidence of genomic and non-genomic regulation of lipogenic and
631 oxidative pathways. *J Biol Chem* **280,** 35983–35991.

632 Demerath EW, Sun SS, Rogers N, Lee M, Reed D, Choh AC, Couch W,
633 Czerwinski SA, Cameron Chumlea W, Siervogel RM & Towne B (2007).
634 Anatomical patterning of visceral adipose tissue: Race, sex, and age
635 variation. *Obesity* **15,** 2984–2993.

636 Dolphin AC (2016). Voltage-gated calcium channels and their auxiliary
637 subunits: physiology and pathophysiology and pharmacology. *J*
638 *Physiol* **594,** 5369–5390.

639 Erdogmus S, Concepcion AR, Yamashita M, Sidhu I, Tao AY, Li W, Rocha
640 PP, Huang B, Garippa R, Lee B, Lee A, Hell JW, Lewis RS, Prakriya M &
641 Feske S (2022). Cavβ1 regulates T cell expansion and apoptosis
642 independently of voltage-gated Ca2+ channel function. *Nat Commun*;
643 DOI: 10.1038/s41467-022-29725-3.

644 Fedorenko OA, Pulbutr P, Banke E, Akaniro-Ejim NE, Bentley DC, Olofsson

645 CS, Chan S & Smith PA (2020). CaV1.2 and CaV1.3 voltage-gated L-
646 type Ca2+ channels in rat white fat adipocytes. *J Endocrinol* **244,**
647 369–381.

648 Foryst-ludwig A, Clemenz M, Hohmann S, Hartge M, Sprang C, Frost N,
649 Krikov M, Bhanot S, Barros R, Morani A, Unger T & Kintscher U
650 (2008). Metabolic Actions of Estrogen Receptor Beta (ER b) are
651 Mediated by a Negative Cross-Talk with PPAR c. *PLoS Genet* **4,**
652 e1000108.

653 Grove KL, Fried SK, Greenberg AS, Xiao XQ & Clegg DJ (2010). A
654 microarray analysis of sexual dimorphism of adipose tissues in high-
655 fat-diet-induced obese mice. *Int J Obes* **34,** 989–1000.

656 Heng TSP et al. (2008). The immunological genome project: Networks of
657 gene expression in immune cells. *Nat Immunol* **9,** 1091–1094.

658 Hvarfner A, Bergström R, Lithell H, Mörlin C, Wide L & Ljunghall S (1988).
659 Changes in calcium metabolic indices during long-term treatment of
660 patients with essential hypertension. *Clin Sci* **75,** 543–549.

661 Izawa T, Koshimizu E, Komabayashi T & Tsuboi M (1983). Effects of Ca2+
662 and calmodulin inhibitors on lipolysis induced by epinephrine,
663 norepinephrine, caffeine and ACTH in rat epididymal adipose tissue.
664 *Nihon Seirigaku Zasshi* **45,** 36–44.

665 Jiralerspong S & Goodwin PJ (2016). Obesity and breast cancer prognosis:
666 Evidence, challenges, and opportunities. *J Clin Oncol* **34,** 4203–4216.

667 Kothari C, Diorio C & Durocher F (2020). The importance of breast
668 adipose tissue in breast cancer. *Int J Mol Sci* **21,** 1–33.

669 Kraus RL, Li Y, Gregan Y, Gotter AL, Uebele VN, Fox S V., Doran SM,
670 Barrow JC, Yang ZQ, Reger TS, Koblan KS & Renger JJ (2010). In
671 vitro characterization of T-type calcium channel antagonist TTA-A2
672 and in vivo effects on arousal in mice. *J Pharmacol Exp Ther* **335,**
673 409–417.

674 Mair KM, Gaw R & MacLean MR (2020). Obesity, estrogens and adipose
675 tissue dysfunction – implications for pulmonary arterial hypertension.
676 *Pulm Circ*; DOI: 10.1177/2045894020952023.

677 Martin RL, Lee JH, Cribbs LL, Perez-Reyes E & Hanck DA (2000).
678 Mibefradil block of cloned T-type calcium channels. *J Pharmacol Exp*
679 *Ther* **295,** 302–308.

680 Namkung Y, Kim S, Shin H, Namkung Y, Skrypnyk N, Jeong M, Lee T, Lee
681 M, Kim H, Chin H, Suh P, Kim S & Shin H (2001). Requirement for the
682 L-type Ca 2 + channel α 1D subunit in postnatal pancreatic β cell
683 generation Find the latest version : Requirement for the L-type Ca 2 +
684 channel α 1D subunit in postnatal pancreatic β cell generation. *J Clin*
685 *Invest* **108,** 1015–1022.

686 Newell-Fugate AE (2017). The role of sex steroids in white adipose tissue
687 adipocyte function. *Reproduction* **153,** R133–R149.

688 Oguri A, Tanaka T, Iida H, Meguro K, Takano H, Oonuma H, Nishimura S,
689 Morita T, Yamasoba T, Nagai R & Nakajima T (2010). Involvement of

690 Ca $_V$ 3.1 T-type calcium channels in cell proliferation in mouse
691 preadipocytes. *Am J Physiol Physiol* **298,** C1414–C1423.

692 Parker CR & Mahesh VB (1976). Hormonal events surrounding the natural
693 onset of puberty in female rats. *Biol Reprod* **14,** 347–353.

694 Pfaffl MW (2001). A new mathematical model for relative quantification in
695 real-time RT-PCR. *Nucleic Acids Res* **29,** 16–21.

696 Qiu J, Bosch MA, Jamali K, Xue C, Kelly MJ & Rønnekleiv OK (2006).
697 Estrogen upregulates T-type calcium channels in the hypothalamus
698 and pituitary. *J Neurosci* **26,** 11072–11082.

699 Reverchon M, Ramé C, Bertoldo M & Dupont J (2014). Adipokines and the
700 Female Reproductive Tract. *Int J Endocrinol* **18,** 2014.

701 Schorr M, Dichtel LE, Gerweck A V., Valera RD, Torriani M, Miller KK &
702 Bredella MA (2018). Sex differences in body composition and
703 association with cardiometabolic risk. *Biol Sex Differ* **9,** 1–10.

704 Sims C, Reisenweber S, Viswanathan PC, Choi BR, Walker WH & Salama
705 G (2008). Sex, age, and regional differences in L-type calcium current
706 are important determinants of arrhythmia phenotype in rabbit hearts
707 with drug-induced long QT type 2. *Circ Res* **102,** 86–100.

708 Souza Bomfim GH, Mitaishvili E, Aguiar TF & Lacruz RS (2021). Mibefradil
709 alters intracellular calcium concentration by activation of
710 phospholipase C and IP3 receptor function. *Mol Biomed*; DOI:
711 10.1186/s43556-021-00037-0.

712 Sun C, Qi R, Wang L, Yan J & Wang Y (2012). P38 MAPK regulates
713 calcium signal-mediated lipid accumulation through changing VDR
714 expression in primary preadipocytes of mice. *Mol Biol Rep* **39,** 3179–
715 3184.

716 Sung YJ, Pérusse L, Sarzynski MA, Fornage M, Sidney S, Sternfeld B, Rice
717 T, Terry G, Jacobs DR, Katzmarzyk P, Curran JE, Carr JJ, Blangero J,
718 Ghosh S, Despres J-P, Rankinen T, Rao DC & Bouchard C (2016).
719 Genome-wide association studies suggest sex-specific loci associated
720 with abdominal and visceral fat. *Int J Obes* **40,** 662–674.

721 Uebele VN, Gotter AL, Nuss CE, Kraus RL, Doran SM, Garson SL, Reiss
722 DR, Li Y, Barrow JC, Reger TS, Yang ZQ, Ballard JE, Tang C, Metzger
723 JM, Wang SP, Koblan KS & Renger JJ (2009). Antagonism of T-type
724 calcium channels inhibits high-fat diet-induced weight gain in mice. *J*
725 *Clin Invest* **119,** 1659–1667.

726 Valencak TG, Osterrieder A & Schulz TJ (2017). Sex matters: The effects
727 of biological sex on adipose tissue biology and energy metabolism.
728 *Redox Biol* **12,** 806–813.

729 Wang H, Zhang X, Xue L, Xing J, Jouvin MH, Putney JW, Anderson MP,
730 Trebak M & Kinet JP (2016). Low-Voltage-Activated CaV3.1 Calcium
731 Channels Shape T Helper Cell Cytokine Profiles. *Immunity* **44,** 782–
732 794.

733 Wang HH, Cui Q, Zhang T, Guo L, Dong MZ, Hou Y, Wang ZB, Shen W, Ma
734 JY & Sun QY (2017). Removal of mouse ovary fat pad affects sex

735 hormones, folliculogenesis and fertility. *J Endocrinol* **232,** 155–164.

736 De Weille JR, Schweitz H, Maes P, Tartar A & Lazdunski M (1991).
737 Calciseptine, a peptide isolated from black mamba venom, is a
738 specific blocker of the L-type calcium channel. *Proc Natl Acad Sci U S*
739 *A* **88,** 2437–2440.

740 Winn NC, Jurrissen TJ, Grunewald ZI, Cunningham RP, Woodford ML,
741 Kanaley JA, Lubahn DB, Manrique-acevedo C, Rector RS, Vieira-potter
742 XVJ & Padilla J (2023). Estrogen receptor- ⎵ signaling maintains
743 immunometabolic function in males and is obligatory for exercise-
744 induced amelioration of nonalcoholic fatty liver. *Am J Physiol Metab*
745 **316,** 156–167.

746 Yang X, Schadt EE, Wang S, Wang H, Arnold AP, Ingram-Drake L, Drake
747 TA & Lusis AJ (2006). Tissue-specific expression and regulation of
748 sexually dimorphic genes in mice. *Genome Res* **16,** 995–1004.

749 Ying W, Riopel M, Bandyopadhyay G, Dong Y, Birmingham A, Seo JB,
750 Ofrecio JM, Wollam J, Hernandez-Carretero A, Fu W, Li P & Olefsky JM
751 (2017). Adipose Tissue Macrophage-Derived Exosomal miRNAs Can
752 Modulate in Vivo and in Vitro Insulin Sensitivity. *Cell* **171,** 372-
753 384.e12.

754 Zamponi GW, Striessnig J, Koschak A & Dolphin AC (2015). The
755 physiology, pathology, and pharmacology of voltage-gated calcium
756 channels and their future therapeutic potential. *Pharmacol Rev* **67,**
757 821–870.

758 Zhang C, Bosch MA, Rick EA, Kelly MJ & Rønnekleiv OK (2009). 17beta;-
759 estradiol regulation of T-type calcium channels in gonadotropin-
760 releasing hormone neurons. *J Neurosci* **29,** 10552–10562.

761 Zhang F, Ye J, Meng Y, Ai W, Su H, Zheng J, Liu F, Zhu X, Wang L, Gao P,
762 Shu G, Jiang Q & Wang S (2018). Calcium supplementation enhanced
763 adipogenesis and improved glucose homeostasis through activation of
764 camkii and PI3K/Akt signaling pathway in porcine bone marrow
765 mesenchymal stem cells (pBMSCs) and mice fed high fat diet (HFD).
766 *Cell Physiol Biochem* **51,** 154–172.

767 Zhang Y, Xie L, Gunasekar SK, Tong D, Mishra A, Gibson WJ, Wang C,
768 Fidler T, Marthaler B, Klingelhutz A, Dale Abel E, Samuel I, Smith JK,
769 Cao L & Sah R (2017). SWELL1 is a regulator of adipocyte size, insulin
770 signalling and glucose homeostasis. *Nat Cell Biol* **19,** 504–517.

771

772

Table 1. PCR/qPCR primers used for amplification of voltage-gated Ca^{2+} channel and housekeeping genes.

Gene	Forward Primer	Reverse Primer	Annealing temperature (°C)
TATA-box	CAGCCTTCCACCTTATGCTC	TGCTGCTGTCTTTGTTGCTC	63
GAPDH	GGCAAGTTCAATGGCACAGT	TGGTGAAGACGCCAGTAGACTC	63
Pgk_1	TAGTGGCTGAGATGTGGCACAG	GCTCACTTCCTTTCTCAGGCAG	63
Cacnca1a	CGTCATCAAACCGGGTACA	GTCGAAGTTGGTGGGAGGAG	62
Cacnca1b	CTCCAGCGTAAACTCACCG	TTGTCCCTATCACGATGCC	62
Cacna1c	CGCATTGTCAATGACACGATC	CGGCAGAAAGAGCCCTTGT	58
Cacna1d	TTGGTACGGACGGCTCTCA	CCCCACGGTTACCTCATCAT	58
Cacnca1e	TGTGTGGCCATCGTTCATCA	TCGGAAGTTGCCCAAACGT	62
Cacnca1f	AGCACAAGACCGTAGTGGTG	ATACCCCCAATGCCACACAG	58
Cacnca1g	TACTTTGGCCGGGGAATC	TCTCCCACACACTGATGACC	58
Cacnca1h	GTGAGTGTACCCGTGAGGACAA	TTTCCTGTGCTGTAGGTGGG	62
Cacnca1i	CGGAAAGCTGGTCTGCAAT	GAACTGAGCTGTGAGCACGAA	62
Cacna1s	GCAGTGCGTGTTTGTTGCTA	ACTCTATCTGCGTGGGGTCT	58

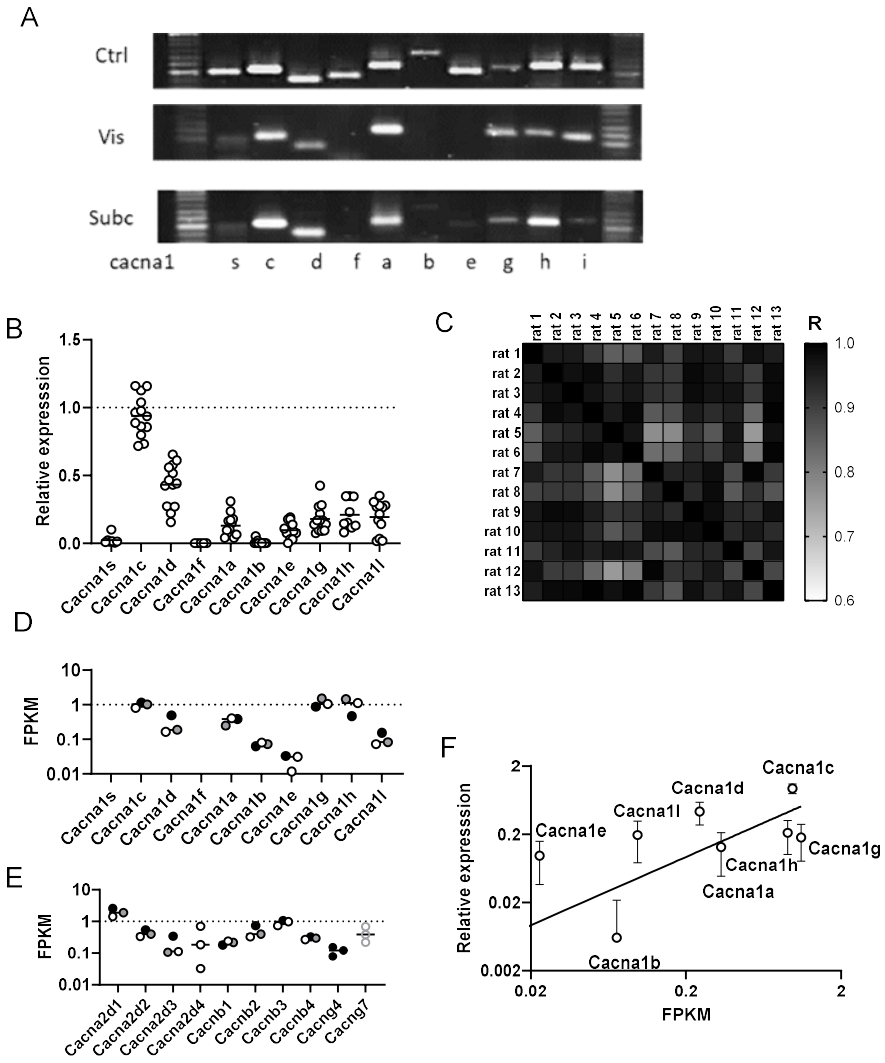

Figure 1. Expression of *Cacna1* genes in isolated adipocytes from purified visceral epididymal adipocytes of adult male rat. A)

Representative RT-PCR products of voltage-dependent L-type calcium channels alpha$_1$ subunits for brain (Ctrl), epididymal fat (Vis) and inguinal subcutaneous fat (Subc). Key: Ctrl, rat brain; Vis, epididymal; Subc, inguinal subcutaneous fat; *Cacna1s* (CaV1.1); *Cacna1c* (CaV1.2); *Cacna1d* (CaV1.3); *Cacna1f* (CaV1.4); *Cacna1a* (CaV2.1); *Cacna1b* (CaV2.2); *Cacna1e* (CaV2.3); *Cacna1g* (CaV3.1); *Cacna1h* (CaV3.2); *Cacna1i* (CaV3.3). B) Relative expression of CaV alpha$_1$ subunits in male epididymal visceral fat as determined by qPCR normalized to mRNA expression of CaV1.2; key as for (A) (n = 5-13). C) Pearson correlation matrix generated for the qPCR expression profiles of the 11 CaV genes as indicated in (B) for the epididymal fat pads of 13 different male rats. Significant correlation ($p<0.05$) was seen for all qPCR data sets indicative of reproducibility between animals. R values are coded as shown ~~C~~D) RNA-seq data of CaV alpha$_1$ subunits expressed as Fragments Per Kilobase of transcript per Million mapped reads (FPKM). Key as for (A). Each point is data from the epididymal adipocytes of a different animal. Only data with a Geometric mean of >0.1 is shown. ~~D~~E) RNA-seq data in FPKM of CaV accessory subunits. Key: $\alpha_2\delta$ subunits *Cacna2d1, Cacna2d2*, *Cacna2d3* and *Cacna2d4*; β subunits *Cacnb1*, *Cacnb2*, *Cacnb3* and *Cacnb4*; ϒ *Cacng*4 and *Cacng*7. Each point is data from the epididymal adipocytes of a different animal. Only data with a Geometric mean of >0.1 is shown. ~~E) Pearson correlation matrix generated for the qPCR expression profiles of the 11 CaV genes as indicated in (B) for the epididymal fat pads of 13 different male rats. Significant correlation~~

~~(p<0.05) was seen for all qPCR data sets indicative of reproducibility between animals. R values are coded as shown~~ F) Linear relationship between the relative expression of the 8 highest expressed CaV genes determined by qPCR with FPKM (>0.02) from RNA-seq. Data are means ± SD. Line is a best fit with linear regression with a slope, R (p=0.0002), of 0.46 (0.16 to 0.77, 95% C.I.).

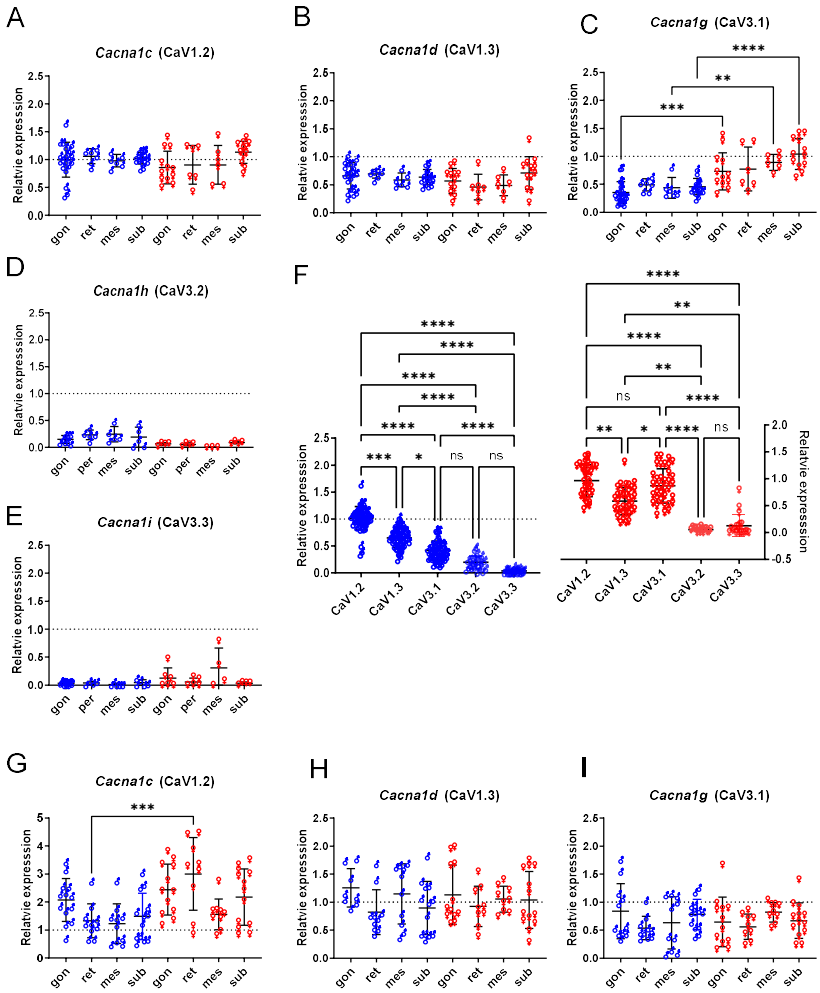

Figure 2. Cacna1g genes show differential expression between male and female fat depots of adult rat. Expression of five CaV genes: *Cacna1c* (A, G), *Cacna1d* (B, H), *Cacna1g* (C, I), *Cacna1h* (D) and *Cacna1i* (E) in different fat depots for males (♂) and females (♀) of adult

Formatted: Normal (Web), Justified, Space After: 6 pt

P>140 (A-F) and juvenile P14-P30 (G-I) rats. F) Relative expression of the genes indicated pooled from the four different depots for males (♂) and females (♀) of adult P>140 rats. Key: gon, gonadal fat, epididymal for males or periovarian for females; ret, retroperitoneal fat; mes, mesenteric fat; sub, IWAT. Data are normalized to mRNA expression of CaV1.2 male epididymal adipocytes. Statistical significance is by One-way ANOVA, with Sidak multiple comparison test. For D, E and F, statistical significance is by Kruskal-Wallis with Dunn's multiple comparison test. Each point represents a sample from a different animal; for adults n = 6-20, juveniles n = 8-13

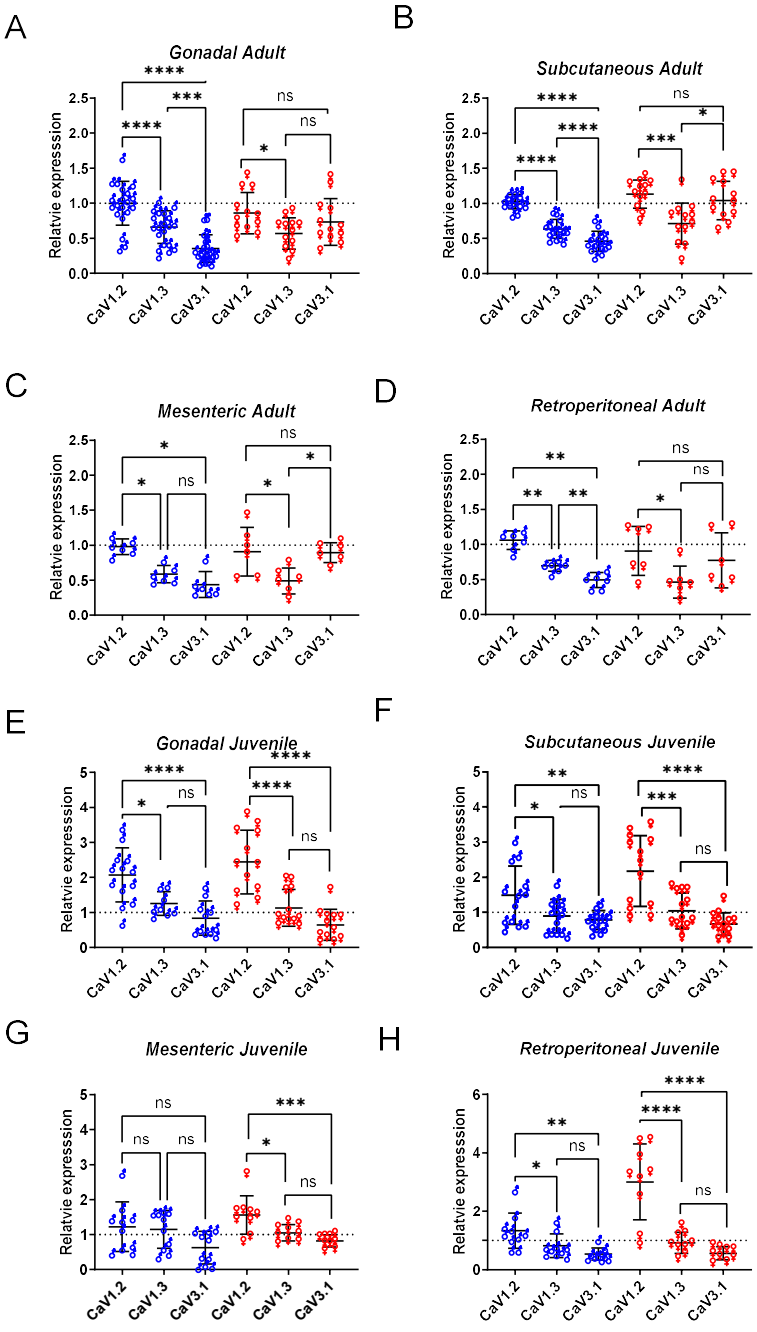
A
Gonadal Adult
B
Subcutaneous Adult
C
Mesenteric Adult
D
Retroperitoneal Adult
E
Gonadal Juvenile
F
Subcutaneous Juvenile
G
Mesenteric Juvenile
H
Retroperitoneal Juvenile
Relatvie expresssion
Relatvie expression
CaV1.2
CaV1.3
CaV3.1
ns

Figure 3. Cacna1 genes show similar rank order of expression in fat depots of juveniles and adult male but not adult female rat. Expression of the three CaV genes: *Cacna1c* (CaV1.2), *Cacna1d* (CaV1.3) and *Cacna1g* (CaV3.1) in different fat depots for males (♂) and females (♀) of adult P>140 (A, B, C, D) and juvenile P14-P30 (E, F, G, H) rats as indicated. Data are normalized to mRNA expression of CaV1.2 in male epididymal adipocytes. Due to the relatively low expression of CaV3.2 and CaV3.3 these are omitted for clarity. Statistical significance is by One-way ANOVA, with Tukey multiple comparison test. Each point represents a sample from a different animal; for adults n = 6-20, juveniles n = 8-13.

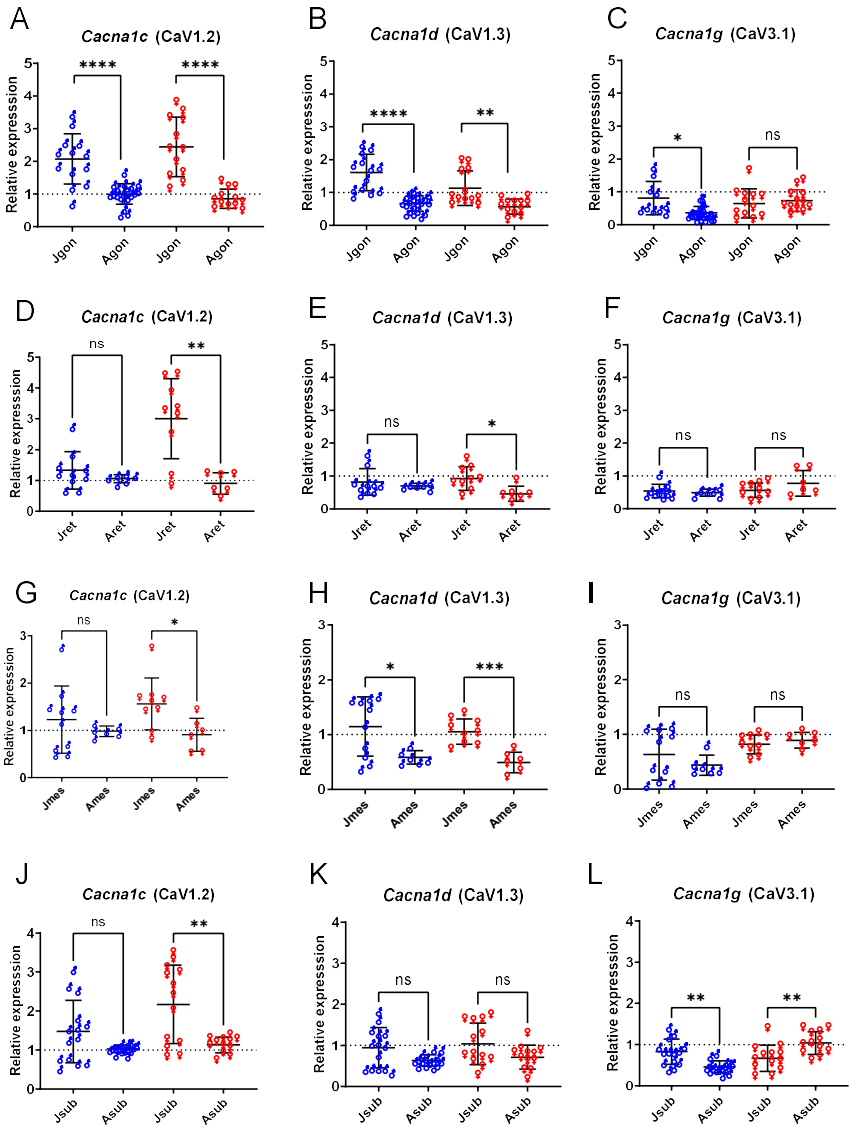

Figure 4. Cacna1 genes show changes in expression with age. Expression of the three CaV genes: *Cacna1c* (A, D, G, J), *Cacna1d* (B, E,

H, K) and *Cacna1g* (C, F, I, L) in different fat depots for males (♂) and females (♀) from juvenile P14-P30 (J prefix) and adult P>140 (A prefix) rats. Key: gon, gonadal fat (A, B, C), epididymal for males or periovarian for females; ret, retroperitoneal fat (D, E, F); mes, mesenteric fat (G, H, I); sub, IWAT (J, K, L). Data are normalized to mRNA expression of CaV1.2 from male epididymal adipocytes. Statistical significance is by Welch's ANOVA, with Dunnett's T3 comparison test ~~with significance at P of < 0.01 to account for statistical comparisons performed on this data in Fig 2~~. Each point represents a sample from a different animal; for adults n = 6-20, juveniles n = 8-13.

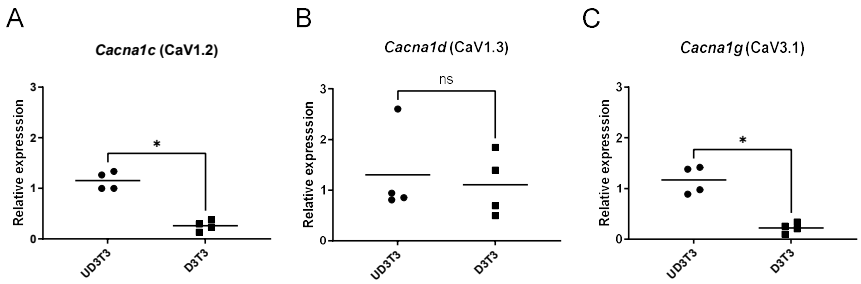

Figure 5. Expression of *Cacna1* genes in 3T3-L1 cells is affected by differentiation. Expression of the three CaV genes: *Cacna1c* (A), *Cacna1d* (B) and *Cacna1g* (C) in undifferentiated (UD3T3) and differentiated (D3T3) 3T3-L1 cells. Data are normalized to mRNA expression of CaV1.2 in epididymal fat. Statistical significance is by Mann Whitney. Each point represents a sample from a different passage number (n = 4). There we no significant change in the coefficient of variation (Paired t-test)

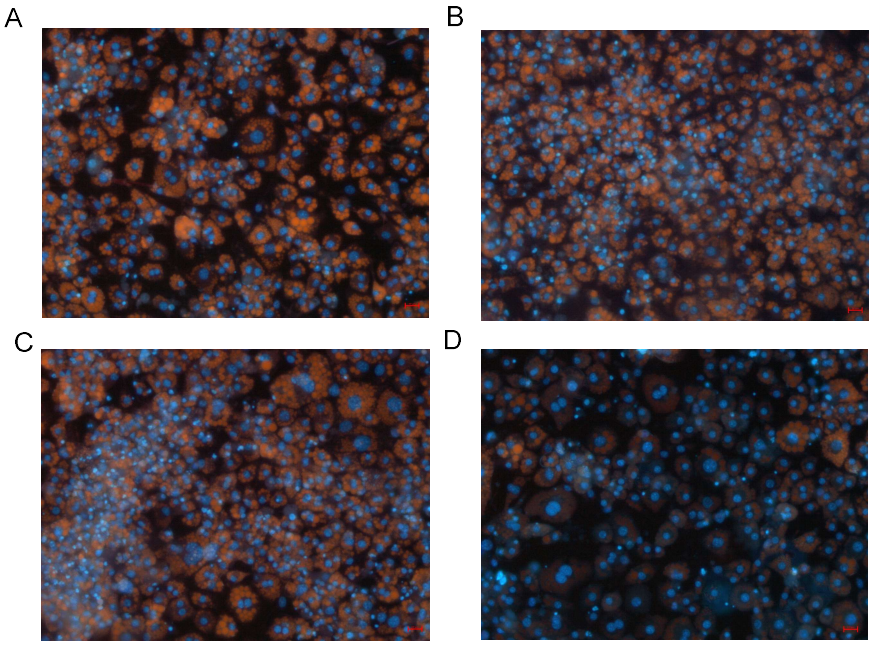

Figure 6. Images of differentiated 3t3-L1 adipocytes stained with Hoechst 33342 and Nile red in the presence of CaV blockers. A) Control, B) 10 μM mibefradil, C) 50 μM TTA-A2, D) 10 nM calciseptine. Cells were incubated for 8 days in drugs and vehicle control. Scale bar 10 μM.

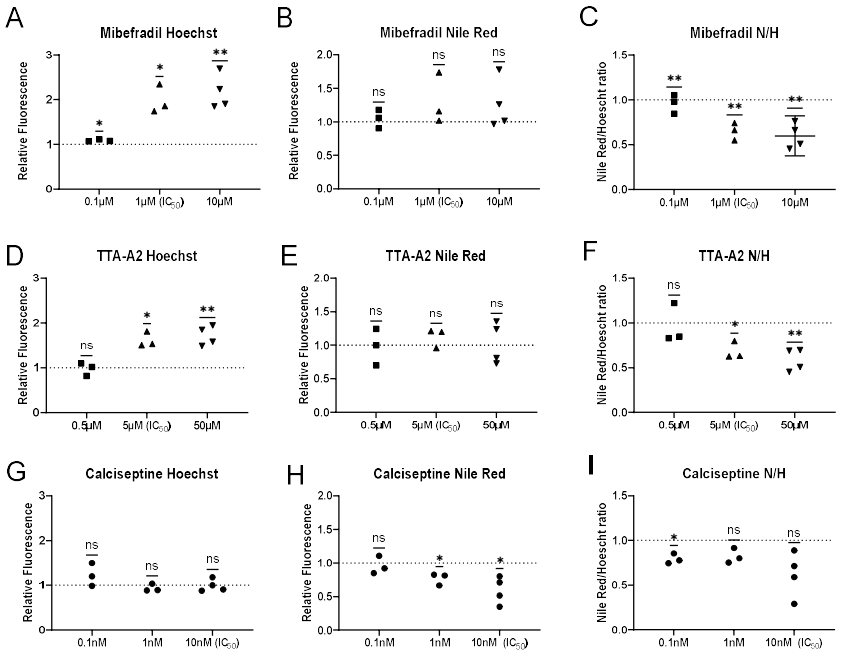

Figure 7. Inhibition of CaV3.1 promotes pre-adipocyte proliferation but does not affect adipocyte differentiation. Effect of CaV blockers on cell proliferation measured by staining with Hoechst, differentiation measured by staining with Nile red and adipogenesis by the ratio of Nile red to Hoechst staining (N/H). Fluorescence values for drugs are normalised (Relative fluorescence) to their respective vehicle control: DMSO for mibefradil and TTA-A2, water for calciseptine. Statistical significance is by One-sample test. Each point represents a sample from a different passage number (n = 3-4).

887